Exploring Sensitized Photon Upconversion – From Past to Present

Colette M. Sullivan and Lea Nienhaus§*

§Grammaticakis-Neumann Prize 2023

Abstract: The conversion of low energy photons into high energy photons *via* triplet-triplet annihilation (TTA) photon upconversion (UC) has become a promising avenue for furthering a wide range of optoelectronic applications. Through the decades of research, many combinations of triplet sensitizer species and annihilator molecules have been investigated unlocking the entire visible spectrum upon proper pairings of sensitizer and annihilator identities. Here, we reflect upon the seminal works which lay the foundation for TTA-UC originating from solution-based methods and highlight the recent advances made within the solid state primarily focusing on perovskite-based triplet generation.

Keywords: Energy transfer · Perovskite · Triplet · Upconversion

Colette M. Sullivan received her BSc from the University of South Carolina Aiken in Spring 2021. She then joined the Nienhaus group at Florida State University to pursue her graduate degree in Chemistry. Her research interests include exploring upconversion in perovskite-sensitized systems using a variety of structural and optical characterization methods.

Dr. Lea Nienhaus received her BSc from the Universität Ulm in 2010 and her PhD in Chemistry from the University of Illinois at Urbana-Champaign in 2015 working with Martin Gruebele. After her postdoctoral work with Moungi Bawendi at MIT, she began her independent career at Florida State University in 2018. Current research directions in the Nienhaus lab focus on triplet generation at hybrid inorganic/organic interfaces. A combination of optical spectroscopy and scanning probe microscopy enables a unique understanding of the complex photophysical processes occurring in these systems.

1. Introduction

First observed by Parker and Hatchard in 1960,[1] 'delayed fluorescence' or upconversion (UC) has become an exciting emerging field, with the potential to alleviate the current global energy crisis by developing green energy sources. To date, there are many available mechanisms of UC, including the climbing of the 'ladder-like' energy levels of lanthanides,[2] second harmonic frequency generation,[3–5] and triplet-triplet annihilation (TTA).[6–8] Due to the energy storage in the long-lived spin-triplet states, efficient TTA-UC is possible under low, solar relevant powers ideal for solar-related applications.[9] Generally, TTA-UC is achieved by a combination of a sensitizer and annihilator species due to the

Correspondence: Dr. L. Nienhaus, E-mail: nienhaus@rice.edu
Department of Chemistry, Rice University, Houston, TX-77005

spin-forbidden nature of direct excitation from the ground state to triplet excited state, outlined in Fig. 1. Incident low energy light is solely absorbed by the sensitizer species and the energy is subsequently transferred to the annihilator molecule. Upon interaction of two annihilator molecules with populated spin-triplets, the spin-allowed TTA-UC mechanism yields one annihilator in the electronic ground state and the second annihilator as an excited singlet state. Upon radiative recombination of the excited singlet state, the upconverted photon with an apparent anti-Stokes shift is produced.
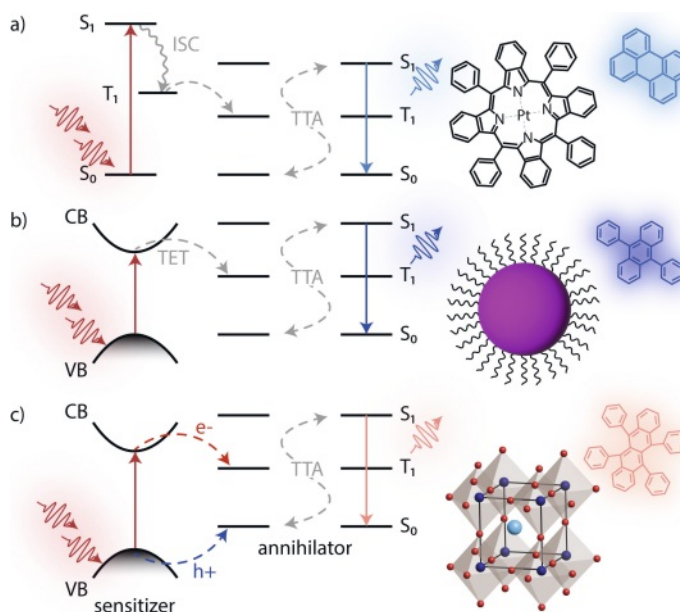

Fig. 1. Different methods of achieving TTA-UC with a) metal-organic complexes, b) nanocrystals, and c) bulk perovskite triplet sensitizers.

In this review article, we reflect on the beginnings of TTA-UC and current developments from the solution foundation to the current state-of-the-art solid-state bilayers – *i.e.* the history of photon upconversion from past to present (Fig. 2).

Fig. 2. Illustration of the photon upconversion timeline beginning with metalorganic complexes, then to nanocrystals, and perovskites and transition metal dichalcogenides TMDs.

Table 1. Names and structures for referenced annihilators

Name (abvr.)	Structure
9,10-diphenylanthracene (DPA)	
rubrene	
dibenzotetraphenylperiflanthene (DBP)	
1-chloro-9,10-bis(phenylethynyl)anthracene (1-CBPEA)	
naphtho[2,3-a]pyrene (NaPy)	

1.1 Foundation for TTA-UC

The foundation of current UC research was laid by Castellano and coworkers in 2005,[9] who utilized metal-organic complexes paired with anthracene annihilators in solution-based UC systems. In these systems, metal-organic complexes commonly containing late series transition metals (Ru,[9,10] Pd,[11–13] Zn,[14] Ir[15]), act as the triplet sensitizer. Within these sensitizer complexes, the heavy metal facilitates intersystem crossing (ISC) from the excited singlet state to the lowest excited triplet state. The formed triplet excited state can then transfer to nearby annihilator molecules (Fig. 1a). These seminal works by Castellano[9,10,15,16] and Baluschev et al.[12,17,18] realized the potential for TTA-UC by laying the foundation of the understanding of the underlying processes.[19]

In early studies by Castellano and coworkers, the authors found Ru(II)-based sensitizers paired with 9,10-diphenylanthracene (DPA) (Table 1) and anthracene yielded efficient green-to-blue TTA-UC at low powers.[9,16] Some key findings from their work are the potential to utilize TTA-UC as a low power UC mechanism achievable with non-coherent excitation sources (*i.e.* visible to the naked eye) and the ability for TTA to drive bimolecular cycloadditions of anthracenes. By exchanging the DPA annihilator with anthracene within their solution UC system resulted in a significant decrease to the overall system due to anthracene dimerization.[16,20] However, during the sensitization process, multiple excited states can be accessed leading UC as a potential method for selectively driving photochemical reactions which typically require high energy ultraviolet irradiation. Despite the low UC yields, the study highlights the potential for TTA systems to be an avenue for achieving efficient photocatalysis.[21–24]

1.2 Nanocrystal Sensitization

The next explored avenue for triplet sensitization was semiconductor nanocrystal-based (NC) sensitization. Due to spin mixing between the triplet and singlet excitonic states, the ISC step is not required for triplet energy transfer to occur, thus minimizing associated energy losses. NCs also exhibit a high degree of customizability through both composition and degree of quantum confinement resulting in direct control of bandgaps ranging from the near-infrared (NIR) to visible.[25–27] In addition, NCs generally have high PLQYs[28] with narrow emission bandwidths,[29] and in conjunction with their facile synthetic methods,[27] make exceptional solution triplet sensitizers.

Lead chalcogenides were the first NCs implemented for both charge transfer from organic chromophores and UC systems.[30–32] In order to remain colloidally stable, NCs require surface passivating ligands for colloidal stability, a problem unique to NC-based triplet sensitization methods. In general, these passivating ligand bind to the NC surface through polar carboxylic or phosphonic acid groups, but also serve as tunneling barrier ultimately reducing the degree of energy transfer.[33] In an early study by Huang et al., two modes of triplet energy transfer were investigated: i) the NC was passivated as per usual with the bulk organic ligands; and ii) additional mediating, anthracene-based ligands were utilized.[31] Utilizing PbSe NC sensitizers with rubrene in method one resulted in successful NIR-to-yellow TTA-UC despite the electrically inert organic ligands decorating the NC surface, albeit with low yields. Changing the ligand chemistry and introducing 9-anthracene carboxylic acid (ACA) to mediate the exciton transfer from a CdSe NC to DPA, the authors were able to significantly increase the UC photoluminescence quantum yield (PLQY) and achieve green-to-blue TTA-UC.

Altering the morphology of the NC serves as a method for tuning the UC process. Relaxing the degree of quantum confinement for the NC from 0D (quantum dots) to 1D (nanorods) or 2D (nanoplatelets) can lead towards a wide degree of anisotropic properties, potentially serving as a steppingstone for future solid-state applications. Studies by VanOrman et al. have shown that successful green-to-blue UC can be achieved by 2D CdSe nanoplatelets.[34] Here, the exciton is quantumly confined within the thickness of the nanoplatelet allowing for an overall larger surface area for both native and transmitter ACA ligands to bind.[35] Similarly, 1D CdTe nanorods can serve as effective sensitizers for red-to-blue TTA-UC.[36]

1.3 Perovskite-Sensitized TTA-UC

Another widely popular triplet sensitizer species are organic-inorganic lead halide perovskites (LHPs).[6,7,37,38] With the general ABX_3 crystal structure, compositional tunability can be achieved with relative ease, thus allowing a vast range of suitable LHP compositions to be synthesized in the near-infrared (NIR) region of the electromagnetic spectrum. These materials have become popular for photovoltaic applications due to their favorable charge diffusion lengths, long lifetimes, and solution processability.[39–41] Perovskite-sensitized UC comes both in form of excitonic nano-

crystal-based triplet sensitization[42–46] and in form of non-excitonic bulk perovskite-based charge transfer. The first example of LHP NCs as triplet sensitizers was reported by Mase *et al.* in 2017 where 3D CsPbBr$_3$ NCs paired with DPA resulted in green-to-blue TTA-UC.[44] Other seminal works by the Wu,[42,45,47] Yanai,[43,46] and Kimizuka[43,46] groups have shown that not only are LHP NCs viable candidates for efficient sensitizers, they are also able to expand the range of TTA-UC into the ultraviolet regime.[45,46]

2. Bulk Perovskite-Senstized TTA-UC

Utilization of bulk LHPs as solid-state triplet sensitizers results in an asynchronous charge transfer mechanism as the generated electron and holes are not bound in form of an exciton but are present as free charges (Fig. 1c). Following charge transfer, the charges recombine to form the bound triplet state.

First reported by Nienhaus *et al.* in 2019, NIR-to-visible TTA-UC can be achieved utilizing LHPs with a rubrene:dibenzotetraphenylperiflanthene (DBP) annihilator:emitter combination.[7] Here, a mixed cation LHP of methylammonium (MA) and formamidinium (FA) (MA$_{0.15}$FA$_{0.85}$PbI$_3$, MAFA) perovskite was successfully paired with a rubrene annihilator doped with ~1% DBP (rubreneDBP). The inclusion of DBP had been observed to increase the overall quantum yield of rubrene films in the solid state, and in the UC process, acts as a Förster resonance energy transfer (FRET) acceptor.[48,49] Up until this 2019 study, achieving high UCQYs within the solid-state had remained a challenge using the aforementioned systems due to limitations in the NIR absorbance due to limited exciton transport through the PbS NC film,[33,50] and from this study, multiple investigations into the underlying process began.

Variations to the underlying LHP thickness holds promise to tuning the success of LHP sensitized TTA-UC. To this point, Wieghold, *et. al* in 2019 investigated the impact of LHP thickness.[6] Again, MAFA perovskites were utilized with the rubreneDBP annihilator layer. The authors found that indeed, increasing the MAFA thickness ultimately lowers the characteristic intensity threshold (I_{th}) of TTA-UC, *i.e.* the point where TTA becomes the dominant decay pathway leading to efficient UC. These results also suggest that the charge transfer to the rubreneDBP annihilator/emitter pair directly competes with trap filling, a detrimental nonradiative pathway.

2.1 *Mechanistic Insights*

To elucidate the impact of DBP on the UC process of the solution-processed solid-state LHP/rubreneDBP devices, Wieghold *et. al* investigated the role of DBP doping. They varied the percentage of DBP within the MAFA/rubrene bilayer systems (0% to 5.5%).[48] As expected, with larger amounts of DBP present within the organic semiconductor (OSC) layer, increased FRET from rubrene to DBP results in a decrease to the rubrene emission (Fig. 3a). Within the bilayer device, the authors interestingly observed little beneficial impact of larger amounts of DBP as all fabricated bilayers exhibited similar UCPL yields (Fig. 3b,c).

Diving deeper into the beneficial nature of DBP doping, Bossanyi *et. al.* investigated the interplay of DBP within rubrene nanocrystal thin films.[51] DBP had been originally proposed as a beneficial dopant for UC methods due to competition of FRET with the singlet fission (SF) process thus improving the TTA yields. The authors here report that DBP does not outcompete SF (~10 ps timescale) but rather mitigates the triplet pair separation ^{1}(T...T). Here, DBP acts as a funnel for the generated rubrene singlets on the order of ~50 ps, thus extracting the singlets faster than the triplet pair state ^{1}(TT) can dissociate (~140 ps, Fig. 3d). As less energy is lost through non-radiative pathways, *e.g.* triplet-quenching, the authors observed a 20-fold increase of the PL quantum yield.

Within the LHP bilayers, charge extraction must occur across the interface emphasizing the role of underlying traps, defect
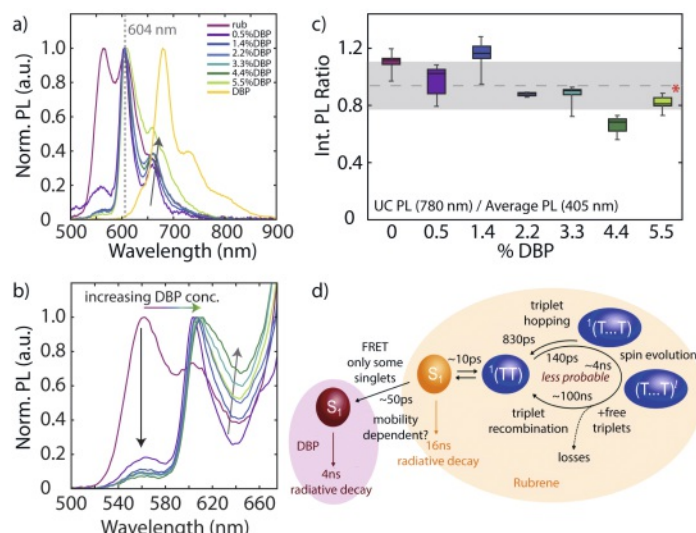

Fig. 3. a) Normalized photoluminescence (PL) under 405 nm excitation of the doped rubreneDBP OSCs. The grey arrow highlights the increase of the 680 nm shoulder indicative of DBP aggregation. b) Normalized UCPL of the doped MAFA/rubreneDBP bilayers under 780 nm excitation. The black arrow highlights the decrease of the rubrene PL feature at 565 nm. c) Box and whisker plot of the UCPL intensities normalized by the direct PL. The dashed grey line and shaded area indicate the mean and the region of uncertainty, respectively. Reprinted (adapted) with permission from ref. [44]. Copyright **2020** *American Chemical Society*. d) Schematic of the role of DBP doping within rubrene nanocrystal films highlighting the interplay of singlet energy collection, singlet fission, and triplet fusion. Reproduced from ref. [47] with permission from the *Royal Society of Chemistry*.

states, and interfacial sites on the UC process. In an effort to determine the exact mechanism governing the LHP free-carrier sensitization, ultrafast transient absorption (TA) investigations by Conti III *et al.* interrogated the interfacial charge transfer between the LHP and rubreneDBP annihilator.[52] Here, FA-rich LHPs (FA$_{0.85}$MA$_{0.15}$PbI$_3$, FAMA) serve as the sensitizer and by selectively pumping the FAMA *via* 700 nm pump, the evolution of rubrene signatures in the 6 ns time window signify successful triplet population within the bilayer. In addition to the rapid sub-nanosecond triplet generation, the authors found evidence for hot-carrier extraction from the FAMA to rubrene.

Surface treatments to the underlying LHP also shed light on the mechanistic steps. 'Cleansing' the LHP surface *via* a post-fabrication solvent treatment had been proposed to both remove unreacted precursors and potentially generate defects and excess PbI$_2$ all of which can impact the underlying properties.

Work by the Nienhaus and Bawendi groups into the influence of a surface solvent treatment has shown that not only does a change to the underlying dopant level occur of the LHP but also to the overall upconversion process.[38,53] Interfacial traps are generated when polar solvents such as isopropanol are utilized as they can readily dissolve the FAI and MAI within the perovskite structure.[38] These films also exhibit an increase to the UC yields likely due to trap-assisted TTA-UC. Upon using solvents which react with FAI or MAI such as toluene, a diminished UC yield is observed due to removal of the halide (I$^-$) from the structure.

Expanding the solvents for the post-fabrication treatment, Sullivan *et al.* found that in addition generating PbI$_2$ at the interface, treatments with polar solvents which interact with the perovskite precursors (Type I) reduce the undesirable delta-phase within the lattice.[53] Here, with the removal of the delta-phase, a larger amount of carriers can participate thus boosting the UC yields. Through scanning tunneling spectroscopy (STS) investigations, the authors also found that the underlying dopant nature of the FAMA perovskite is ultimately altered by preferential ion
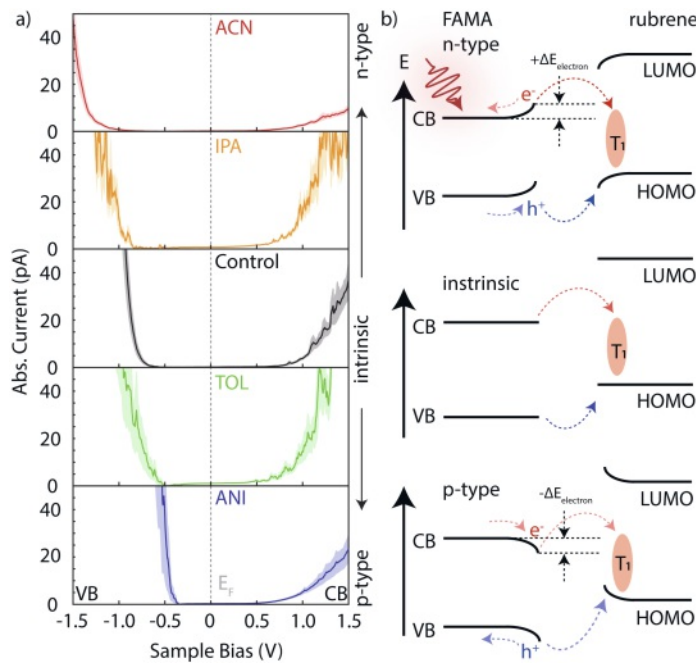
Fig. 4. a) Average STS IV curves for the treated perovskite only films where the shaded region represents the 95 % confidence interval. Dashed grey line represents the Fermi level (E_F). b) Illustration of the interfacial band-bending behaviour of the treated bilayers. Adapted with permission from ref. [49]. Copyright **2022** *John Wiley and Sons*.

removal. Treatments with the Type I solvents result in a *n*-type doping causing upwards band bending at the interface, while the other solvents (no interaction with perovskite precursors - Type II; reacts with precursors – Type III) result in a more *p*-type doping resulting in downwards band bending. Here, the authors proposed a more detailed view of the charge injection from the FAMA to the rubrene annihilator, outlined in Fig. 4b.

Other mechanistic investigations include probing the triplet diffusion within these solid UC bilayers.[54] As both the triplet lifetime and rate of diffusion-mediated TTA are contingent upon the underlying triplet population, investigating the UCPL dynamics is important for furthering solid-state UC. Two distinctive regimes can be found within the UC PL dynamics within the LHP bilayers – a fast and slow rise. Wieghold *et al.* were able to determine that the dual rise times can be attributed to rapid TTA occurring close to the interface and slow, diffusion mediated TTA occurring further from the interface, respectively. Parasitic back-transfer occurs with high efficiency for the generated rubrene excited singlets by the interface leading to a reduction to the UC yield.

2.2 *Environmental Stressors*

Considering the long-term goal of employment of TTA-UC devices in photovoltaic applications, understanding the impact of environmental stressors on the LHP bilayer is required. Implementation of LHP TTA-UC bilayers for real-word PV applications would require operating under constant irradiation at temperatures up to 80 °C.[55–57] Investigations of the effect of elevated temperatures by Bieber *et al.* show that upon reaching 65 °C, the UC emission diminishes and is non-recoverable (Fig. 5a).[58] Through ultrafast TA spectroscopy, the authors found that charge extraction still occurs at the elevated temperatures (Fig. 5c); however, cooling back to room temperature causes non-uniform morphological changes across the bilayer (Fig. 5b). Locations which remain unaltered (amorphous) successfully undergo UC, but the altered, crystalline regions show no detectable UC emission likely stemming from an increase in SF in rubrene.

On the other end of the spectrum, the effect of temperatures below room temperature have shown to be beneficial for TTA-UC. Sullivan *et al.* investigated MAFA/rubrene bilayers where the UC reaches its maximum efficiency at 170 K.[59] Upon cooling past 170 K, the UC yield steadily decreases despite the PLQY of the rubrene annihilator increasing (Fig. 5d,e). Through a combination of modeling and spectroscopic investigations, the authors found that ultimately the underlying triplet diffusion determines the overall UC QY of the devices (Fig. 5f,g), and highlight the fact that this system could be better suited for applications in lower temperature environments.

The next steps of furthering LHP-sensitized TTA-UC have been exploring other annihilator identities in order to increase the achiev-
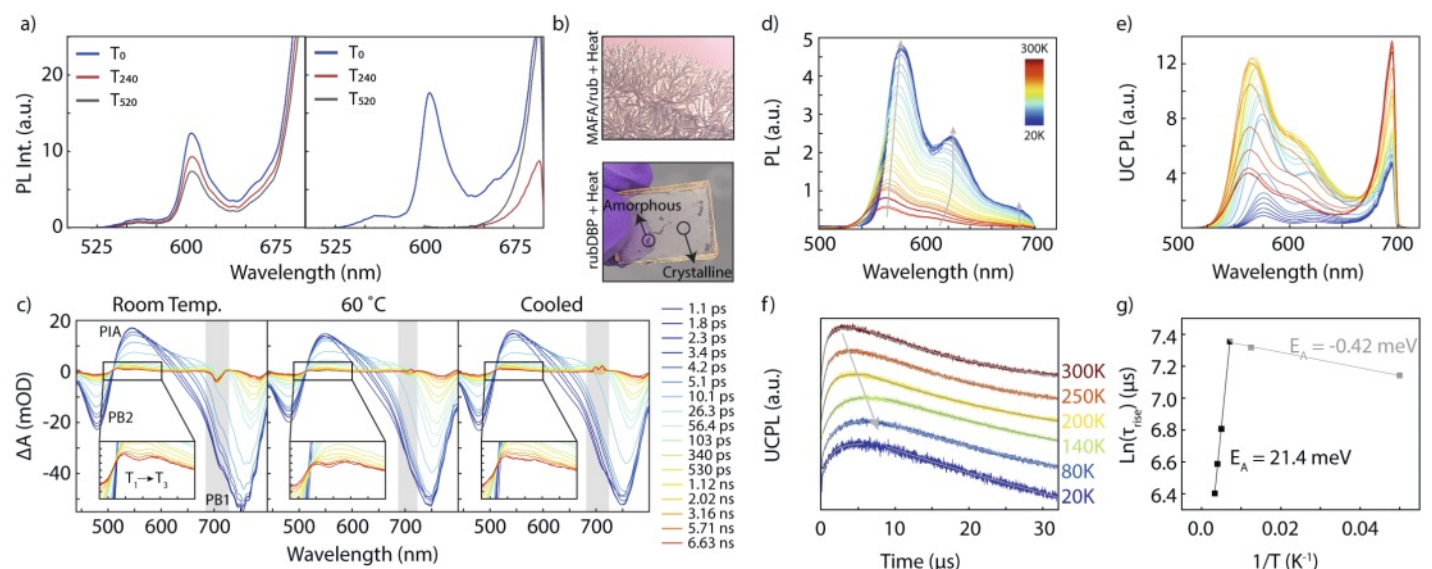

Fig. 5. a) UCPL for a MAFA/rubreneDBP bilayer extracted at select times without (left) and with (right) heating. b) Images of the MAFA/rubreneDBP bilayer and rubreneDBP OSC post-heating. c) Transient absorption spectra extracted at selected delays for the MAFA/rubreneDBP bilayer collected under 700 nm pump at multiple temperatures. Characteristic perovskite photoinduced absorption (PIA) and bleach (PB1, PB2) features have been labelled for clarity. Spectral inserts highlight the $T_1 \rightarrow T_3$ rubrene transition indicative of successful triplet population. The grey boxes denote excess pump scatter. Reprinted (adapted) with permission from ref. [54]. Copyright **2023** *American Chemical Society*. d) Direct PL of a MAFA/rubrene bilayer collected from 300 K to 20 K collected in increments of 10 K. A 700 nm short-pass filter was used to isolate the dye emission. e) UCPL for a MAFA/ rubrene bilayer in the same temperature range. f) UCPL dynamics for the MAFA/rubrene bilayer, offset for clarity. g) Triplet rise times extracted from the UCPL dynamics in f) in an Arrhenius plot. Reproduced from ref. [55] with permission from the *Royal Society of Chemistry*.

able anti-Stokes shift and minimize losses. Due to the ~0.4 eV mismatch of the LHP band energies to that of the T_1 state of rubrene (1.14 eV),[51] exploring annihilators with a $T_1 \sim 1.5$ eV would allow for the most efficient TTA capable within these bilayers as the perovskite bandgap. However, intermolecular coupling effects such as excimer formations and aggregation formation must be taken into consideration. Hence, in-depth investigations into solid-state behaviors of potential annihilators are required to be screened. To this end, recent work from the Nienhaus group has identified suitable solid-state annihilators for LHP-sensitized TTA-UC.[60,61]

2.3. *Annihilators Beyond Rubrene*

From the polyacene family, Sullivan *et al.* found that 1-chloro-9,10-bis(phenylethynyl)anthracene (1-CBPEA) is a suitable solid-state annihilator within the LHP bilayer device configuration resulting in NIR-to-green UC (Fig. 6a).[60] Despite lower PLQYs than the established rubreneDBP annihilator, the authors found that the previously discussed mechanism holds true for this new configuration. Ultrafast charge extraction and triplet formation occurs on the same sub-nanosecond time scales as in rubrene. Considering the I_{th} values of the two bilayers, here the rubreneDBP remains superior with the lower threshold of the two (Fig. 6b). However, upon investigating the UC PL dynamics, drastic differences to the rates of triplet diffusion are seen (Fig. 6c). The previously observed dual rise and slow decay of rubrene are not seen within 1-CBPEA bilayer but rather, a single rise of 28 ns and quick decay are seen. Piecing the information together, the authors determined that despite the outperformance of rubrene to that of 1-CBPEA, 1-CBPEA holds potential to outperform rubrene in the future due to a higher probability of TTA.
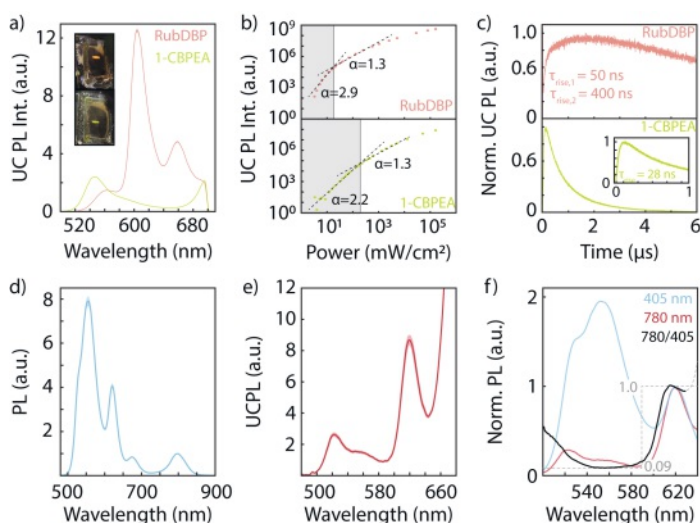

Fig. 6. a) UCPL from a FAMA/RubDBP (pink) and FAMA/1-CBPEA (green) bilayer. b) Power-dependent UCPL for the RubDBP (top, pink) and 1-CBPEA (bottom, green) bilayer devices. Calculated intensity threshold I_{th} values for RubDBP and 1-CBPEA films are 18.2 mW cm^{-2} and 195 mW cm^{-2}, respectively. c) UCPL dynamics for the FAMA/RubDBP (top, pink) and FAMA/1-CBPEA (bot. green) bilayers with a magnification of the early time (1 μs) included for the 1-CBPEA rise. Reproduced from ref. [56] with permission from the *Royal Society of Chemistry*. d) Direct PL from a CsFA/NaPy bilayer collected across four locations on the bilayer, and e) UCPL emission from the NaPy bilayer collected across ten spots. f) Spectra ratio (black) of the direct PL (405 nm) to the UCPL (780 nm) normalized to the 620 nm aggregate feature. Reprinted (adapted) with permission from ref. [57] Copyright **2023** *American Chemical Society*.

The aforementioned intermolecular coupling within the solid-state can be clearly seen for the next novel annihilator for solid-state UC: naphtho[2,3-a]pyrene (NaPy).[61] In the thin-film form,

NaPy exhibits a prominent red-shifted absorption feature not observed in solution, as well as a red-shifted PL feature which has not been previously reported. In this study, a cesium-based perovskite was used in place of the less stable methylammonium containing FAMA LHP ($Cs_{0.09}FA_{0.91}PbI_3$, CsFA). NaPy additionally exhibits excitation wavelength-dependent emission behavior within the bilayer where direct excitation results in the domination of a high energy S_1' emissive state while under 780 nm excitation, the lower energy S_1'' state dominates (Fig. 6d,e,f). These two distinctive states suggest that the underlying differences between the two excitation wavelengths can be attributed to aggregate-induced lowering of the singlet state. Populating the lower S_1'' state from the ^{1}(TT) results in thermodynamically favorable TTA-UC thus explaining its prominence with the UC spectra. Generating the higher energy S_1' state is only possible then *via* endothermic TTA-UC, hence why it appears diminished compared to the direct excitation spectrum.

3. Conclusions

Since its initial discovery, photon upconversion has come a long way. Original discoveries from the early solution-based studies with metal-organic complex sensitizers laid the groundwork for understanding the underlying principles of TTA. In the next chapter, NC-sensitized TTA-UC, we find TTA-UC can occur across the electromagnetic spectrum, however limitations were found due to poor exciton diffusion in NC films. Transitioning from solution to solid state, bulk LHPs have been shown to be successful sensitizers for solid-state UC. As the focus shifts from fine-tuning the underlying LHP to discovering new suitable annihilators, we can look to the future. Beyond thin films, LHP single crystals are also suitable as triplet-sensitizers.[62] Single crystals hold promise for heterogeneous catalysis applications where the LHP crystal facets can serve as a catalysis location to thus populate reactant triplet states. Looking beyond LHP sensitizers, van der Waals heterostructures such as transition metal dichalcogenides (TMDs) have been used as triplet sensitizers.[63] Here, 2D WSe$_2$ or MoSe$_2$ monolayers are crafted and when interfaced with rubreneDBP, successful NIR-to-orange TTA-UC occurs.[64,65] Across the many different avenues of established photon upconversion methods, future work will include expanding the solid-state annihilator library and development of solid-state sensitizers thus continuing the photon upconversion narrative.

Table 2. Abbreviations

TTA	triplet-triplet annihilation
UC	upconversion
CB	conduction band
VB	valence band
ISC	intersystem crossing
DPA	9,10-diphenylanthracene
NC	nanocrystal
NIR	near-infrared
PLQY	photoluminescence quantum yield
LHP	lead halide perovskite
DBP	dibenzotetraphenylperiflanthene
FRET	Förster resonance energy transfer
TA	transient absorption
SF	singlet fission
PV	photovoltaic
1-CBPEA	1-chloro-9,10-bis(phenylethynyl)anthracene
FAMA	formamidinium (85%) methylammonium (15%) lead triiodide
MAFA	methylammonium (85%) formamidinium (15%) lead triiodide
CsFA	Cesium (9%) formamidinium (91%) lead triiodide

[1] C. A. Parker, C. G. Hatchard, E. J. Bowen, *Pro. R. soc. Lond. Ser. A. Math. Phys. Sci.* **1997**, *269*, 574, https://doi.org/10.1098/rspa.1962.0197.

[2] M.-F. Joubert, *Opt. Mater.* **1999**, *11*, 181, https://doi.org/10.1016/S0925-3467(98)00043-3.

[3] N. Thantu, *J. Lumin.* **2005**, *111*, 17, https://doi.org/10.1016/j.jlumin.2004.06.002.

[4] N. M. Lawandy, R. L. MacDonald, *J. Opt. Soc. Am. B, JOSAB* **1991**, *8*, 1307, https://doi.org/10.1364/JOSAB.8.001307.

[5] E. V. Makeev, S. E. Skipetrov, *Opt. Commun.* **2003**, *224*, 139, https://doi.org/10.1016/S0030-4018(03)01756-5.

[6] S. Wieghold, A. S. Bieber, Z. A. VanOrman, L. Daley, M. Leger, J.-P. Correa-Baena, L. Nienhaus, *Matter.* **2019**, *1*, 705, https://doi.org/10.1016/j.matt.2019.05.026.

[7] L. Nienhaus, J.-P. Correa-Baena, S. Wieghold, M. Einzinger, T.-A. Lin, K. E. Shulenberger, N. D. Klein, M. Wu, V. Bulović, T. Buonassisi, M. A. Baldo, M. G. Bawendi, *ACS Energy Lett.* **2019**, *4*, 888, https://doi.org/10.1021/acsenergylett.9b00283.

[8] W. Wu, H. Guo, W. Wu, S. Ji, J. Zhao, *J. Org. Chem.* **2011**, *76*, 7056, https://doi.org/10.1021/jo200990y.

[9] R. R. Islangulov, D. V. Kozlov, F. N. Castellano, *Chem. Commun.* **2005**, 3776, https://doi.org/10.1039/B506575E.

[10] T. N. Singh-Rachford, F. N. Castellano, *Inorg. Chem.* **2009**, *48*, 2541, https://doi.org/10.1021/ic802114d.

[11] V. Yakutkin, S. Aleshchenkov, S. Chernov, T. Miteva, G. Nelles, A. Cheprakov, S. Baluschev, *Chem. Eur. J.* **2008**, *14*, 9846, https://doi.org/10.1002/chem.200801305.

[12] S. Baluschev, V. Yakutkin, T. Miteva, G. Wegner, T. Roberts, G. Nelles, A. Yasuda, S. Chernov, S. Aleshchenkov, A. Cheprakov, *New J. Phys.* **2008**, *10*, 013007, https://doi.org/10.1088/1367-2630/10/1/013007.

[13] R. R. Islangulov, J. Lott, C. Weder, F. N. Castellano, *J. Am. Chem. Soc.* **2007**, *129*, 12652, https://doi.org/10.1021/ja075014k.

[14] S. K. Sugunan, U. Tripathy, S. M. K. Brunet, M. F. Paige, R. P. Steer, *J. Phys. Chem. A* **2009**, *113*, 8548, https://doi.org/10.1021/jp9034776.

[15] W. Zhao, F. N. Castellano, *J. Phys. Chem. A* **2006**, *110*, 11440, https://doi.org/10.1021/jp064261s.

[16] R. R. Islangulov, F. N. Castellano, *Angew. Chem. Int. Ed.* **2006**, *45*, 5957, https://doi.org/10.1002/anie.200601615.

[17] S. Baluschev, T. Miteva, V. Yakutkin, G. Nelles, A. Yasuda, G. Wegner, *Phys. Rev. Lett.* **2006**, *97*, 143903, https://doi.org/10.1103/PhysRevLett.97.143903.

[18] S. Baluschev, P. E. Keivanidis, G. Wegner, J. Jacob, A. C. Grimsdale, K. Müllen, T. Miteva, A. Yasuda, G. Nelles, *Appl. Phys. Lett.* **2005**, *86*, 061904, https://doi.org/10.1063/1.1857073.

[19] T. W. Schmidt, F. N. Castellano, *J. Phys. Chem. Lett.* **2014**, *5*, 4062, https://doi.org/10.1021/jz501799m.

[20] H. Bouas-Laurent, A. Castellan, J.-P. Desvergne, R. Lapouyade, *Chem. Soc. Rev.* **2000**, *29*, 43, https://doi.org/10.1039/A801821I.

[21] S.-Y. Hwang, D. Song, E.-J. Seo, F. Hollmann, Y. You, J.-B. Park, *Sci. Rep.* **2022**, *12*, 9397, https://doi.org/10.1038/s41598-022-13406-8.

[22] B. D. Ravetz, A. B. Pun, E. M. Churchill, D. N. Congreve, T. Rovis, L. M. Campos, *Nature* **2019**, *565*, 343, https://doi.org/10.1038/s41586-018-0835-2.

[23] S. N. Sanders, T. H. Schloemer, M. K. Gangishetty, D. Anderson, M. Seitz, A. O. Gallegos, R. C. Stokes, D. N. Congreve, *Nature* **2022**, *604*, 474, https://doi.org/10.1038/s41586-022-04485-8.

[24] J. Alves, J. Feng, L. Nienhaus, T. W. Schmidt, *J. Mater. Chem. C* **2022**, *10*, 7783, https://doi.org/10.1039/D1TC05659J.

[25] L. E. Brus, *J. Chem. Phys.* **1984**, *80*, 4403, https://doi.org/10.1063/1.447218.

[26] A. L. Efros, L. E. Brus, *ACS Nano* **2021**, *15*, 6192, https://doi.org/10.1021/acsnano.1c01399.

[27] C. B. Murray, D. J. Norris, M. G. Bawendi, *J. Am. Chem. Soc.* **1993**, *115*, 8706, https://doi.org/10.1021/ja00072a025.

[28] A. Caron, G. Noirbent, D. Gigmes, F. Dumur, J. Lalevée, *Macromol. Rapid Commun.* **2021**, *42*, 2100047, https://doi.org/10.1002/marc.202100047.

[29] J. Zhou, M. Zhu, R. Meng, H. Qin, X. Peng, *J. Am. Chem. Soc.* **2017**, *139*, 16556, https://doi.org/10.1021/jacs.7b07434.

[30] M. Tabachnyk, B. Ehrler, S. Gélinas, M. L. Böhm, B. J. Walker, K. P. Musselman, N. C. Greenham, R. H. Friend, A. Rao, *Nature Mater.* **2014**, *13*, 1033, https://doi.org/10.1038/nmat4093.

[31] Z. Huang, X. Li, M. Mahboub, K. M. Hanson, V. M. Nichols, H. Le, M. L. Tang, C. J. Bardeen, *Nano Lett.* **2015**, *15*, 5552, https://doi.org/10.1021/acs.nanolett.5b02130.

[32] M. Wu, D. N. Congreve, M. W. B. Wilson, J. Jean, N. Geva, M. Welborn, T. Van Voorhis, V. Bulović, M. G. Bawendi, M. A. Baldo, *Nature Photon* **2016**, *10*, 31, https://doi.org/10.1038/nphoton.2015.226.

[33] L. Nienhaus, M. Wu, N. Geva, J. J. Shepherd, M. W. B. Wilson, V. Bulović, T. Van Voorhis, M. A. Baldo, M. G. Bawendi, *ACS Nano* **2017**, *11*, 7848, https://doi.org/10.1021/acsnano.7b02024.

[34] Z. A. VanOrman, A. S. Bieber, S. Wieghold, L. Nienhaus, *Chem. Mater.* **2020**, *32*, 4734, https://doi.org/10.1021/acs.chemmater.0c01354.

[35] Z. A. VanOrman, R. Weiss, A. S. Bieber, B. Chen, L. Nienhaus, *Chem. Commun.* **2023**, *59*, 322, https://doi.org/10.1039/D2CC04694F.

[36] Z. A. VanOrman, C. R. I. Conti, G. F. Strouse, L. Nienhaus, *Chem. Mater.* **2021**, *33*, 452, https://doi.org/10.1021/acs.chemmater.0c04468.

[37] A. S. Bieber, Z. A. VanOrman, S. Wieghold, L. Nienhaus, *J. Chem. Phys.* **2020**, *153*, 084703, https://doi.org/10.1063/5.0021973.

[38] L. Wang, J. J. Yoo, T.-A. Lin, C. F. Perkinson, Y. Lu, M. A. Baldo, M. G. Bawendi, *Adv. Mater.* **2021**, *33*, 2100854, https://doi.org/10.1002/adma.202100854.

[39] S. D. Stranks, G. E. Eperon, G. Grancini, C. Menelaou, M. J. P. Alcocer, T. Leijtens, L. M. Herz, A. Petrozza, H. J. Snaith, *Science* **2013**, *342*, 341, https://doi.org/10.1126/science.1243982.

[40] S. D. Stranks, V. M. Burlakov, T. Leijtens, J. M. Ball, A. Goriely, H. J. Snaith, *Phys. Rev. Appl.* **2014**, *2*, 034007, https://doi.org/10.1103/PhysRevApplied.2.034007.

[41] G. Xing, N. Mathews, S. Sun, S. S. Lim, Y. M. Lam, M. Grätzel, S. Mhaisalkar, T. C. Sum, *Science* **2013**, *342*, 344, https://doi.org/10.1126/science.1243167.

[42] S. He, Y. Han, J. Guo, K. Wu, *J. Phys. Chem. Lett.* **2022**, *13*, 1713, https://doi.org/10.1021/acs.jpclett.2c00088.

[43] K. Okumura, N. Yanai, N. Kimizuka, *Chem. Lett.* **2019**, *48*, 1347, https://doi.org/10.1246/cl.190473.

[44] K. Mase, K. Okumura, N. Yanai, N. Kimizuka, *Chem. Commun.* **2017**, *53*, 8261, https://doi.org/10.1039/C7CC03087H.

[45] S. He, X. Luo, X. Liu, Y. Li, K. Wu, *J. Phys. Chem. Lett.* **2019**, *10*, 5036, https://doi.org/10.1021/acs.jpclett.9b02106.

[46] M. Koharagi, N. Harada, K. Okumura, J. Miyano, S. Hisamitsu, N. Kimizuka, N. Yanai, *Nanoscale* **2021**, *13*, 19890, https://doi.org/10.1039/D1NR06588B.

[47] R. Lai, Y. Sang, Y. Zhao, K. Wu, *J. Am. Chem. Soc.* **2020**, *142*, 19825, https://doi.org/10.1021/jacs.0c09547.

[48] S. Wieghold, A. S. Bieber, Z. A. VanOrman, A. Rodriguez, L. Nienhaus, *J. Phys. Chem. C* **2020**, *124*, 18132, https://doi.org/10.1021/acs.jpcc.0c05290.

[49] Y. Zhang, S. R. Forrest, *Phys. Rev. Lett.* **2012**, *108*, 267404, https://doi.org/10.1103/PhysRevLett.108.267404.

[50] N. Geva, L. Nienhaus, M. Wu, V. Bulović, M. A. Baldo, T. Van Voorhis, M. G. Bawendi, *J. Phys. Chem. Lett.* **2019**, *10*, 3147, https://doi.org/10.1021/acs.jpclett.9b01058.

[51] D. G. Bossanyi, Y. Sasaki, S. Wang, D. Chekulaev, N. Kimizuka, N. Yanai, J. Clark, *J. Mater. Chem. C* **2022**, *10*, 4684, https://doi.org/10.1039/D1TC02955J.

[52] C. R. Conti III, A. S. Bieber, Z. A. VanOrman, G. Moller, S. Wieghold, R. D. Schaller, G. F. Strouse, L. Nienhaus, *ACS Energy Lett.* **2022**, *7*, 617, https://doi.org/10.1021/acsenergylett.1c02732.

[53] C. M. Sullivan, A. S. Bieber, H. K. Drozdick, G. Moller, J. E. Kuszynski, Z. A. VanOrman, S. Wieghold, G. F. Strouse, L. Nienhaus, *Adv. Opt. Mater.* **2023**, *11*, 2201921, https://doi.org/10.1002/adom.202201921.

[54] S. Wieghold, A. S. Bieber, Z. A. VanOrman, L. Nienhaus, *J. Phys. Chem. Lett.* **2019**, *10*, 3806, https://doi.org/10.1021/acs.jpclett.9b01526.

[55] S. Wieghold, A. S. Bieber, M. Mardani, T. Siegrist, L. Nienhaus, *J. Mater. Chem. C* **2020**, *8*, 9714, https://doi.org/10.1039/D0TC02103B.

[56] M. V. Khenkin, E. A. Katz, A. Abate, G. Bardizza, J. J. Berry, C. Brabec, F. Brunetti, V. Bulović, Q. Burlingame, A. Di Carlo, R. Cheacharoen, Y.-B. Cheng, A. Colsmann, S. Cros, K. Domanski, M. Dusza, C. J. Fell, S. R. Forrest, Y. Galagan, D. Di Girolamo, M. Grätzel, A. Hagfeldt, E. von Hauff, H. Hoppe, J. Kettle, H. Köbler, M. S. Leite, S. (Frank) Liu, Y.-L. Loo, J. M. Luther, C.-Q. Ma, M. Madsen, M. Manceau, M. Matheron, M. McGehee, R. Meitzner, M. K. Nazeeruddin, A. F. Nogueira, Ç. Odaba?ı, A. Osherov, N.-G. Park, M. O. Reese, F. De Rossi, M. Saliba, U. S. Schubert, H. J. Snaith, S. D. Stranks, W. Tress, P. A. Troshin, V. Turkovic, S. Veenstra, I. Visoly-Fisher, A. Walsh, T. Watson, H. Xie, R. Yıldırım, S. M. Zakeeruddin, K. Zhu, M. Lira-Cantu, *Nat. Energy* **2020**, *5*, 35, https://doi.org/10.1038/s41560-019-0529-5.

[57] M. O. Reese, S. A. Gevorgyan, M. Jørgensen, E. Bundgaard, S. R. Kurtz, D. S. Ginley, D. C. Olson, M. T. Lloyd, P. Morvillo, E. A. Katz, A. Elschner, O. Haillant, T. R. Currier, V. Shrotriya, M. Hermenau, M. Riede, K. R. Kirov, G. Trimmel, T. Rath, O. Inganäs, F. Zhang, M. Andersson, K. Tvingstedt, M. Lira-Cantu, D. Laird, C. McGuiness, S. (Jimmy) Gowrisanker, M. Pannone, M. Xiao, J. Hauch, R. Steim, D. M. DeLongchamp, R. Rösch, H. Hoppe, N. Espinosa, A. Urbina, G. Yaman-Uzunoglu, J.-B. Bonekamp, A. J. J. M. van Breemen, C. Girotto, E. Voroshazi, F. C. Krebs, *Sol. Energy Mater. Sol. Cells* **2011**, *95*, 1253, https://doi.org/10.1016/j.solmat.2011.01.036.

[58] A. S. Bieber, C. M. Sullivan, K. E. Shulenberger, G. Moller, M. Mardani, S. Wieghold, T. Siegrist, L. Nienhaus, *J. Phys. Chem. C* **2023**, *127*, 4773, https://doi.org/10.1021/acs.jpcc.2c08850.

[59] C. M. Sullivan, J. E. Kuszynski, A. Kovalev, T. Siegrist, R. D. Schaller, G. F. Strouse, L. Nienhaus, *Nanoscale* **2023**, *15*, 18832, https://doi.org/10.1039/D3NR04446G.

[60] C. M. Sullivan, L. Nienhaus, *Nanoscale* **2022**, *14*, 17254, https://doi.org/10.1039/D2NR05309H.

[61] C. M. Sullivan, L. Nienhaus, *Chem. Mater.* **2024**, *36*, 1, 417, https://doi.org/10.1021/acs.chemmater.3c02349.

[62] G. Moller, C. M. Sullivan, A. P. Cantrell, M. Mardani, A. S. Bieber, T. Siegrist, L. Nienhaus, *Chem. Mater.* **2024**, https://doi.org/10.1021/acs.chemmater.3c02778.

[63] D. M. de Clercq, J. Yang, M. Hanif, J. Alves, J. Feng, M. P. Nielsen, K. Kalantar-Zadeh, T. W. Schmidt, *J. Phys. Chem. C* **2023**, *127*, 11260, https://doi.org/10.1021/acs.jpcc.3c01682.

[64] R. Dziobek-Garrett, C. J. Imperiale, M. W. B. Wilson, T. J. Kempa, *Nano Lett.* **2023**, *23*, 4837, https://doi.org/10.1021/acs.nanolett.3c00380.

[65] J. Duan, Y. Liu, Y. Zhang, Z. Chen, X. Xu, L. Ye, Z. Wang, Y. Yang, D. Zhang, H. Zhu, *Sci. Adv.* **2022**, *8*, eabq4935, https://doi.org/10.1126/sciadv.abq4935.